

Figure S1. **Replication of identifiability results at different doses of sevoflurane** | (a) Identifiability matrix between wakefulness and post-anaesthetic recovery. (b) Identifiability matrix between wakefulness and vol 2% sevoflurane anaesthesia (right). Entries along the diagonal, represent self-self similarity (correlation of FC patterns), whereas off-diagonal entries represent self-other similarity. (c) Self-self similarity is significantly higher between two conscious states, than between wakefulness and vol 2% sevoflurane. (d) The difference between self-self correlation and mean self-other correlation (differential identifiability) is significantly higher between two conscious states, than between wakefulness and vol 2% sevoflurane. (e) The regional distribution of contributions to identifiability (change in intra-class correlation coefficient) is plotted on the cortical surface. It is significantly spatially correlated with the corresponding map obtained with vol 3% sevoflurane: Spearman $\rho = 0.61$, $p_{spin} < 0.001$, $N = 200$ regions. (f) Identifiability matrix between wakefulness and post-anaesthetic recovery. (g) Identifiability matrix between wakefulness and burst-suppression level of sevoflurane anaesthesia. (h) Self-self similarity is significantly higher between two conscious states, than between wakefulness and burst-suppression level of sevoflurane. (i) The difference between self-self correlation and mean self-other correlation (differential identifiability) is significantly higher between two conscious states, than between wakefulness and burst-suppression level of sevoflurane. (j) The regional distribution of contributions to identifiability (change in intra-class correlation coefficient) is plotted on the cortical surface. It is significantly spatially correlated with the corresponding map obtained with vol 3% sevoflurane: Spearman $\rho = 0.80$, $p_{spin} < 0.001$, $N = 200$ regions. ***, $p < 0.001$.

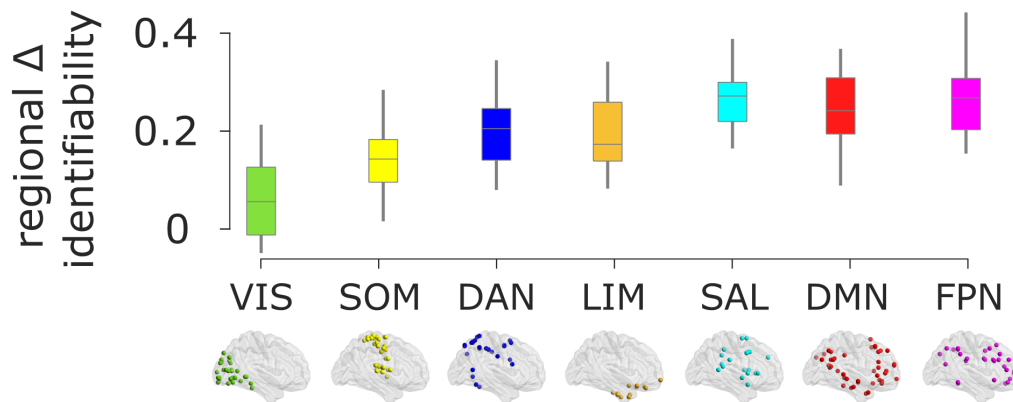


Figure S2. **Regional identifiability across intrinsic connectivity networks** |. SOM, somatomotor network; VIS, visual network; SAL, salience network; DAN, dorsal attention network; FPN, fronto-parietal control network; DMN, default mode network. Box-plots: center line, median; box limits, upper and lower quartiles; whiskers, $1.5 \times$ interquartile range.

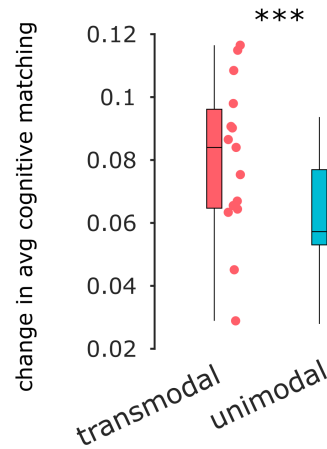


Figure S3. **Change in cognitive matching for unimodal versus transmodal ends of the cortical hierarchy**. NeuroSynth maps were correlated with the archetypal axis map of [83]; maps exhibiting a positive correlation were included at the transmodal end, whereas maps correlating negatively were included at the unimodal end. Box-plot: center line, median; box limits, upper and lower quartiles; whiskers, $1.5 \times$ interquartile range. ***, $p < 0.001$.

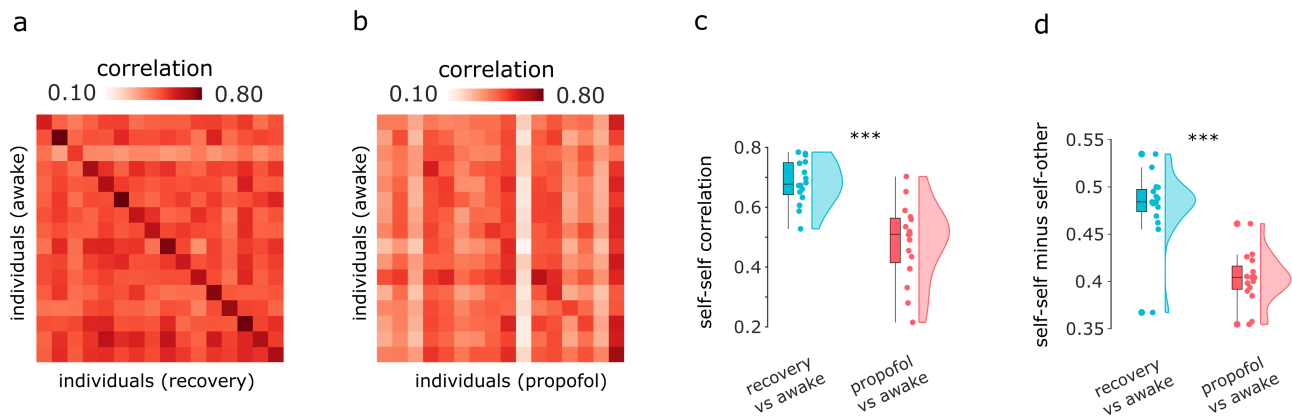


Figure S4. **Identifiability of individual connectomes is diminished under propofol anaesthesia**. (a) Identifiability matrix between wakefulness and post-anaesthetic recovery. (b) Identifiability matrix between wakefulness and propofol anaesthesia (right). Entries along the diagonal, represent self-self similarity (correlation of FC patterns), whereas off-diagonal entries represent self-other similarity. (c) Self-self similarity is significantly higher between two conscious states, than between wakefulness and propofol anaesthesia. (d) The difference between self-self correlation and mean self-other correlation (differential identifiability) is significantly higher between two conscious states, than between wakefulness and propofol anaesthesia. Box-plot: center line, median; box limits, upper and lower quartiles; whiskers, $1.5 \times$ interquartile range. ***, $p < 0.001$.

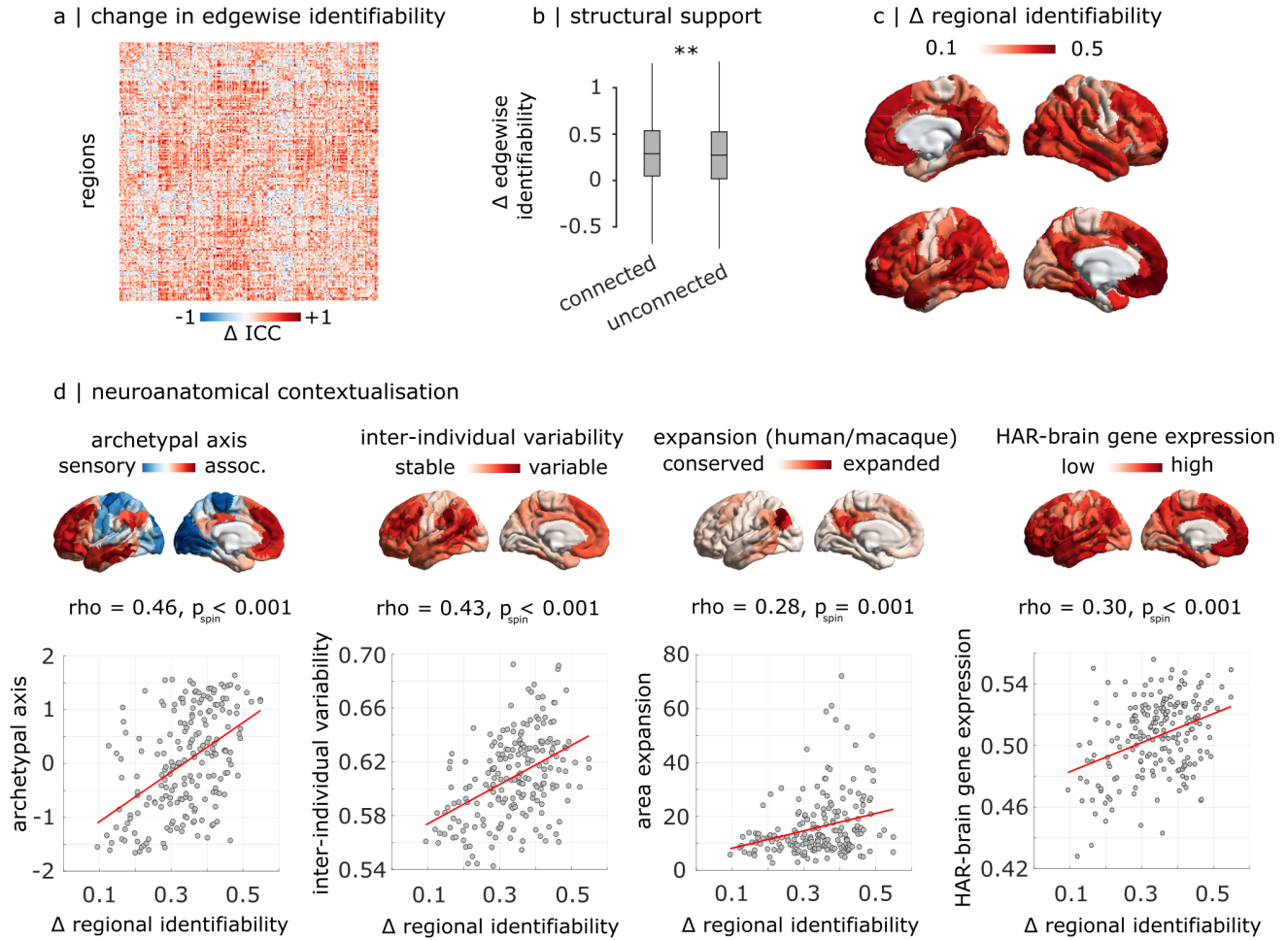


Figure S5. Anatomical characterisation of contributions to propofol-induced loss of identifiability | (a) Edge-level difference in intra-class correlation coefficient between awake-recovery and awake-propofol. (b) The anaesthetic-induced loss of ICC is significantly more pronounced for functional connections with an underlying structural direct connection, than without. Box-plot: center line, median; box limits, upper and lower quartiles; whiskers, $1.5 \times$ interquartile range. **, $p < 0.01$. (c) Regional distribution of propofol-induced loss of ICC, projected onto the cortical surface. It is significantly spatially correlated with the corresponding map obtained with sevoflurane: Spearman $\rho = 0.35$, $p_{spin} < 0.001$, $N = 200$ regions. (d) The propofol-induced regional loss of ICC is significantly spatially aligned with the archetypal sensory-association axis of cortical organisation; the regional distribution of inter-individual variability of functional connectivity; the regional distribution of cortical expansion between macaque and human brains; and the regional expression of human-accelerated genes pertaining to brain function and development (“HAR-brain genes”); $N = 200$ regions

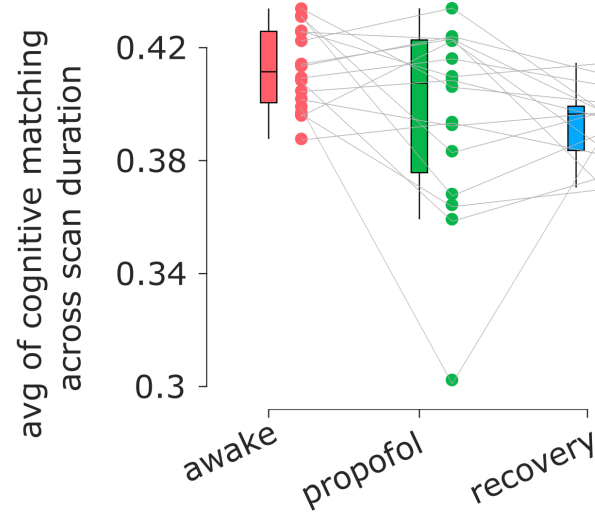


Figure S6. **Cognitive matching from brain activity under wakefulness and propofol anaesthesia** | Ordinate: mean across time of the best decoding score (maximum spatial correlation between brain activity and 123 NeuroSynth meta-analytic maps). *** (black), $p < 0.001$ against wakefulness (FDR-corrected); *** (gray), $p < 0.001$ against recovery (FDR-corrected). Box-plot: center line, median; box limits, upper and lower quartiles; whiskers, $1.5 \times$ interquartile range.

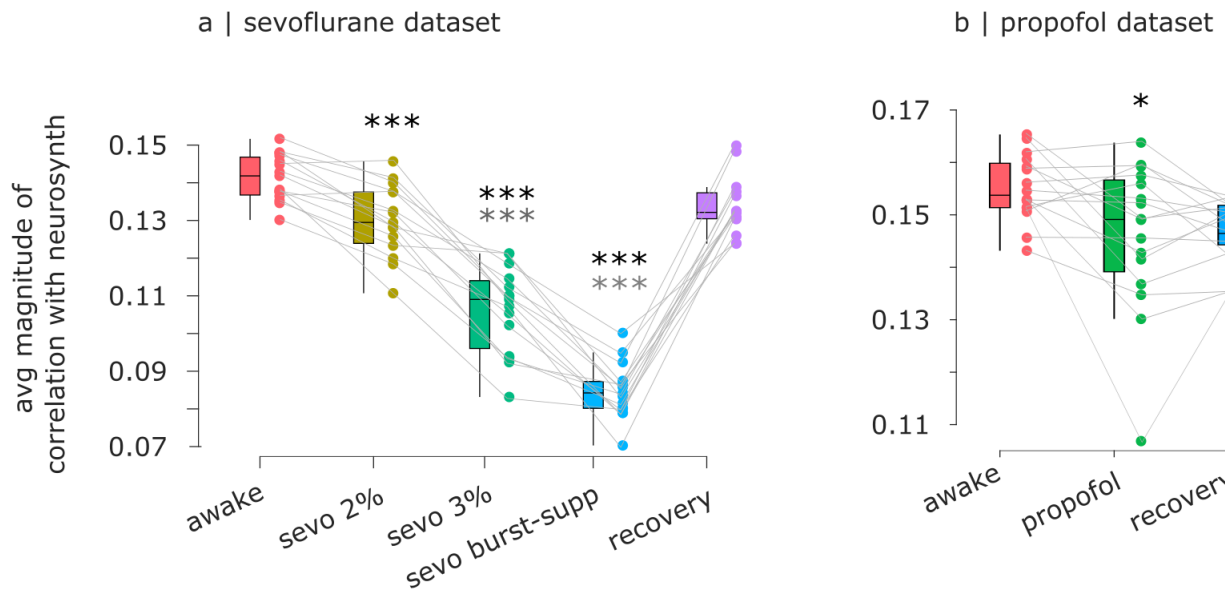


Figure S7. **Alternative quantification of cognitive matching from brain activity under wakefulness and anaesthesia** | (a) Sevoflurane dataset. (b) Propofol dataset. Ordinate: temporal average of the mean absolute value of spatial correlation between brain activity and 123 NeuroSynth meta-analytic maps. *** (black), $p < 0.001$ against wakefulness (FDR-corrected); ** (gray), $p < 0.001$ against recovery (FDR-corrected). Box-plot: center line, median; box limits, upper and lower quartiles; whiskers, $1.5 \times$ interquartile range.

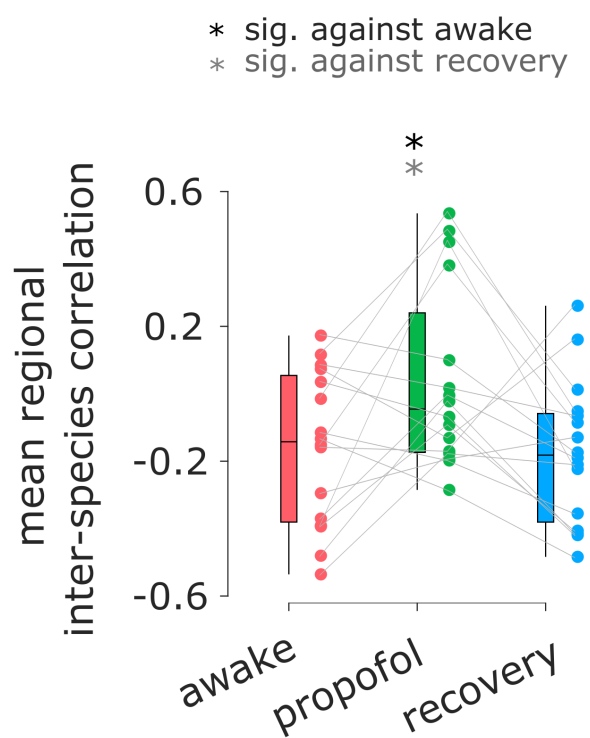


Figure S8. **Human cortical functional connectivity is more similar to macaque cortical connectivity under propofol anaesthesia than during wakefulness** | Ordinate: Regional correlation of mean FC between human and macaque across wakefulness, propofol anaesthesia, and recovery. * (black), $p < 0.05$ against wakefulness (FDR-corrected); * (gray), $p < 0.05$ against recovery (FDR-corrected). Box-plot: center line, median; box limits, upper and lower quartiles; whiskers, $1.5 \times$ interquartile range.

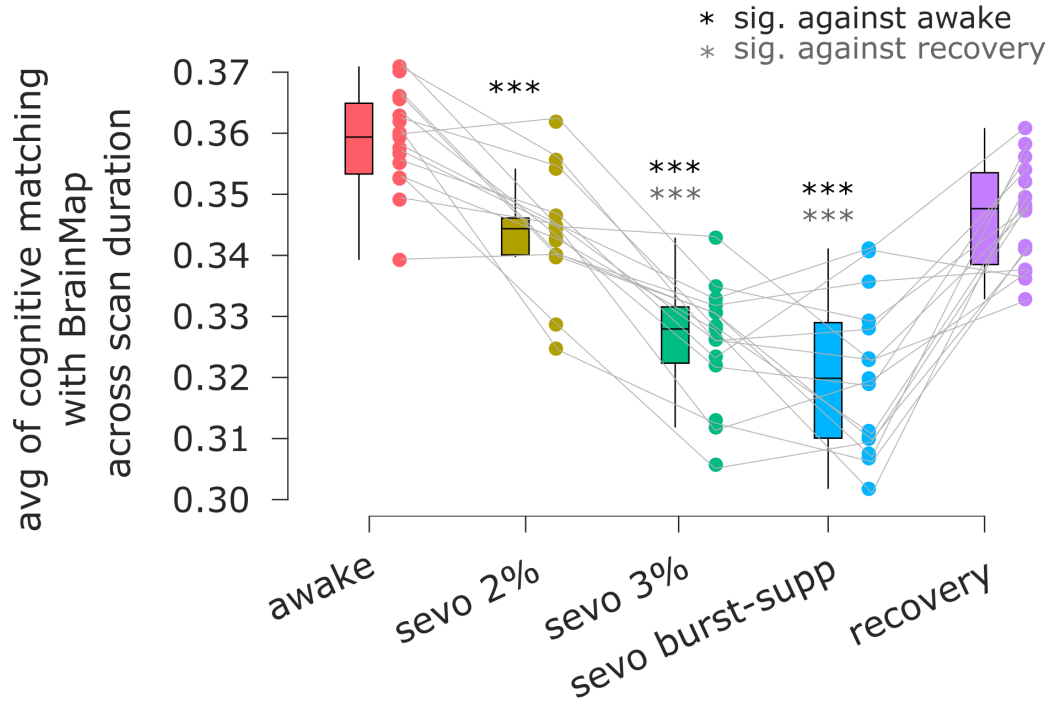


Figure S9. **Replication of decodability results using the BrainMap meta-analytic database** | Ordinate: mean across time of the best decoding score (maximum spatial correlation between brain activity and 66 meta-analytic maps from BrainMap). *** (black), $p < 0.001$ against wakefulness (FDR-corrected); *** (gray), $p < 0.001$ against recovery (FDR-corrected). Box-plot: center line, median; box limits, upper and lower quartiles; whiskers, $1.5 \times$ interquartile range.

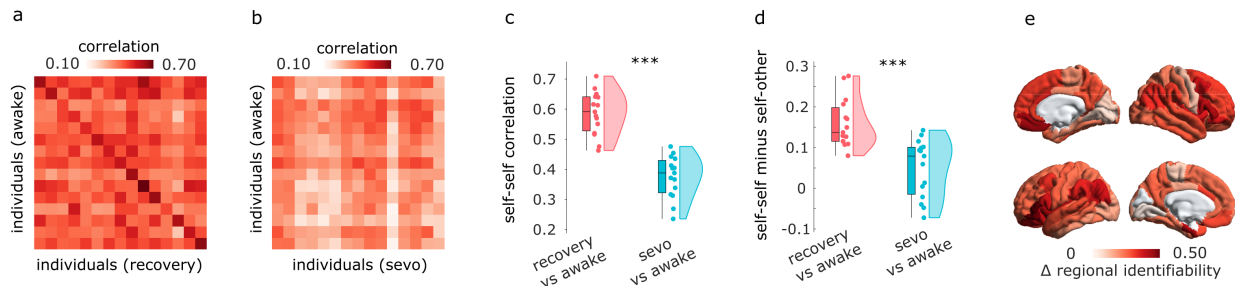


Figure S10. **Identifiability under anaesthesia is robust to parcellation choice** | (a) Identifiability matrix between wakefulness and post-anaesthetic recovery. (b) Identifiability matrix between wakefulness and sevoflurane anaesthesia (right). Entries along the diagonal, represent self-self similarity (correlation of FC patterns), whereas off-diagonal entries represent self-other similarity. (c) Self-self similarity is significantly higher between two conscious states, than between wakefulness and sevoflurane anaesthesia. (d) The difference between self-self correlation and mean self-other correlation (differential identifiability) is significantly higher between two conscious states, than between wakefulness and sevoflurane anaesthesia. (e) The regional distribution of contributions to identifiability (change in intra-class correlation coefficient) is plotted on the cortical surface for the 68 ROIs of the Desikan-Killiany atlas. Box-plot: center line, median; box limits, upper and lower quartiles; whiskers, $1.5 \times$ interquartile range. ***, $p < 0.001$.

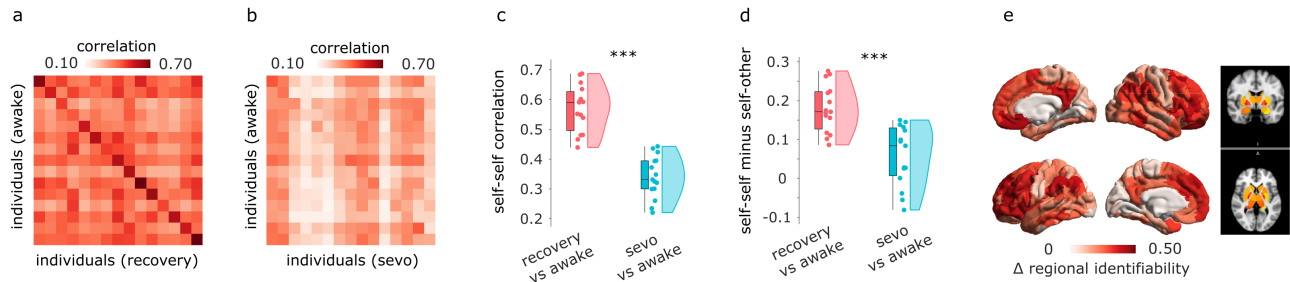


Figure S11. **Identifiability under anaesthesia is robust to inclusion of subcortex** | (a) Identifiability matrix between wakefulness and post-anaesthetic recovery. (b) Identifiability matrix between wakefulness and sevoflurane anaesthesia (right). Entries along the diagonal, represent self-self similarity (correlation of FC patterns), whereas off-diagonal entries represent self-other similarity. (c) Self-self similarity is significantly higher between two conscious states, than between wakefulness and sevoflurane anaesthesia. (d) The difference between self-self correlation and mean self-other correlation (differential identifiability) is significantly higher between two conscious states, than between wakefulness and sevoflurane anaesthesia. (e) The regional distribution of contributions to identifiability (change in intra-class correlation coefficient) is plotted on the cortical surface for the 200-ROIs of the Schaefer atlas, and plotted in volumetric space for the 32 ROIs of the Tian subcortical atlas. Box-plot: center line, median; box limits, upper and lower quartiles; whiskers, $1.5 \times$ interquartile range. ***, $p < 0.001$.

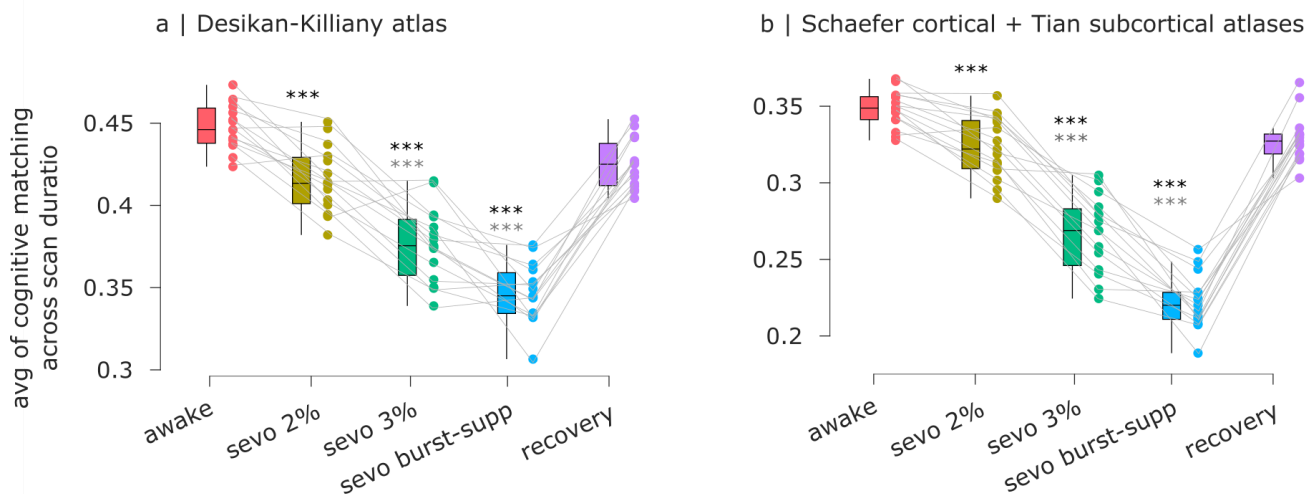


Figure S12. **Decodability of meta-analytic patterns is robust to parcellation choice and inclusion of subcortex** | (a) Results for Desikan-Killiany anatomical parcellation. (b) Results for the combined Schaefer-200 cortical atlas and Tian 32-ROI subcortical atlas. Ordinate: mean across time of the best decoding score (maximum spatial correlation between brain activity and 123 NeuroSynth meta-analytic maps). ***, $p < 0.001$ against wakefulness (FDR-corrected); *** (gray), $p < 0.001$ against recovery (FDR-corrected). Box-plot: center line, median; box limits, upper and lower quartiles; whiskers, $1.5 \times$ interquartile range.

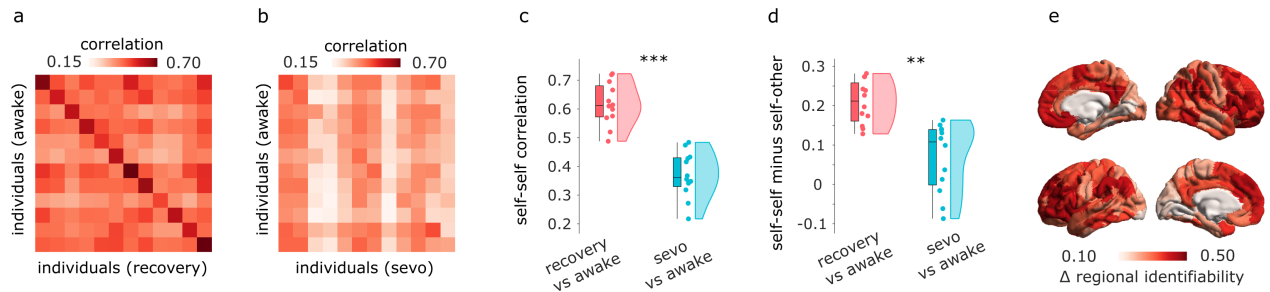


Figure S13. Replication of identifiability results upon excluding high-motion individuals | (a) Identifiability matrix between wakefulness and post-anaesthetic recovery. (b) Identifiability matrix between wakefulness and sevoflurane anaesthesia. Entries along the diagonal, represent self-self similarity (correlation of FC patterns), whereas off-diagonal entries represent self-other similarity. (c) Self-self similarity is significantly higher between two conscious states, than between wakefulness and sevoflurane. (d) The difference between self-self correlation and mean self-other correlation (differential identifiability) is significantly higher between two conscious states, than between wakefulness and sevoflurane. **, $p < 0.01$; ***, $p < 0.001$. (e) The regional distribution of contributions to identifiability (change in intra-class correlation coefficient) is plotted on the cortical surface. It is significantly spatially correlated with the corresponding map obtained when including all individuals: Spearman $\rho = 0.94$, $p_{spin} < 0.001$, $N = 200$ regions.

Contrast	Baseline Mean	Baseline SD	Altered Mean	Null SD	tStat	df	pVal	Eff Size	95% CI Lower	95% CI Upper	Motion corr	Motion pVal
Awake vs Vol 2%	3.81e-01	1.30e-02	3.54e-01	2.33e-02	5.60	14	p < 0.001	1.40	0.96	2.17	-0.01	0.985
Awake vs Vol 3%	3.81e-01	1.30e-02	2.95e-01	2.90e-02	11.24	14	p < 0.001	3.68	2.91	5.38	0.23	0.404
Awake vs Burst-Supp	3.81e-01	1.30e-02	2.36e-01	1.68e-02	28.86	14	p < 0.001	9.28	7.35	13.93	0.27	0.327
Recovery vs Vol 2%	3.61e-01	1.81e-02	3.54e-01	2.33e-02	1.22	14	0.244	0.33	-0.22	0.89	-0.28	0.314
Recovery vs Vol 3%	3.61e-01	1.81e-02	2.95e-01	2.90e-02	8.38	14	p < 0.001	2.61	2.02	3.86	0.07	0.802
Recovery vs Burst-Supp	3.61e-01	1.81e-02	2.36e-01	1.68e-02	20.31	14	p < 0.001	6.85	5.44	10.56	-0.11	0.695

TABLE S1. Statistical results for cognitive matching from NeuroSynth in the sevoflurane dataset.

Contrast	Baseline Mean	Baseline SD	Altered Mean	Null SD	tStat	df	pVal	Eff Size	95% CI Lower	95% CI Upper	Motion corr	Motion pVal
Awake vs Vol 2%	-1.03e-01	2.24e-01	3.86e-03	2.64e-01	-1.39	14	0.186	-0.42	-1.11	0.17	0.30	0.283
Awake vs Vol 3%	-1.03e-01	2.24e-01	2.22e-01	2.42e-01	-3.97	14	0.001	-1.34	-2.45	-0.66	0.32	0.242
Awake vs Burst-Supp	-1.03e-01	2.24e-01	4.86e-01	1.33e-01	-11.16	14	p < 0.001	-3.08	-4.92	-2.25	-0.19	0.490
Recovery vs Vol 2%	-1.31e-02	2.36e-01	3.86e-03	2.64e-01	-0.19	14	0.850	-0.07	-0.76	0.63	0.64	0.012
Recovery vs Vol 3%	-1.31e-02	2.36e-01	2.22e-01	2.42e-01	-3.10	14	0.008	-0.95	-1.81	-0.38	0.63	0.014
Recovery vs Burst-Supp	-1.31e-02	2.36e-01	4.86e-01	1.33e-01	-7.80	14	p < 0.001	-2.51	-4.10	-1.70	0.60	0.020

TABLE S2. Statistical results for human-macaque functional similarity in the sevoflurane dataset.

Contrast	Baseline Mean	Baseline SD	Altered Mean	Null SD	tStat	df	pVal	Eff Size	95% CI Lower	95% CI Upper	Motion corr	Motion pVal
Awake vs Ppfl	4.13e-01	1.44e-02	3.96e-01	3.40e-02	2.03	15	0.061	0.63	0.10	1.17	-0.61	0.014
Recovery vs Ppfl	3.93e-01	1.33e-02	3.96e-01	3.40e-02	-0.38	15	0.710	-0.11	-0.96	0.41	-0.72	0.002

TABLE S3. Statistical results for cognitive matching from NeuroSynth in the propofol dataset.

Contrast	Baseline Mean	Baseline SD	Altered Mean	Null SD	tStat	df	pVal	Eff Size	95% CI Lower	95% CI Upper	Motion corr	Motion pVal
Awake vs Ppfl	-1.60e-01	2.28e-01	3.89e-02	2.71e-01	-2.55	15	0.022	-0.77	-1.35	-0.24	-0.27	0.304
Recovery vs Ppfl	-1.73e-01	2.13e-01	3.89e-02	2.71e-01	-2.83	15	0.013	-0.84	-1.47	-0.29	-0.02	0.935

TABLE S4. Statistical results for human-macaque functional similarity in the propofol dataset

Contrast	Baseline Mean	Baseline SD	Altered Mean	Null SD	tStat	df	pVal	Eff Size	95% CI Lower	95% CI Upper	Motion corr	Motion pVal
Awake vs Vol 2%	4.48e-01	1.40e-02	4.16e-01	1.99e-02	5.97	14	p < 0.001	1.82	1.22	2.91	0.15	0.602
Awake vs Vol 3%	4.48e-01	1.40e-02	3.77e-01	2.24e-02	10.92	14	p < 0.001	3.69	2.85	5.60	0.32	0.248
Awake vs Burst-Supp	4.48e-01	1.40e-02	3.47e-01	1.81e-02	16.32	14	p < 0.001	6.03	4.81	9.13	0.26	0.340
Recovery vs Vol 2%	4.25e-01	1.51e-02	4.16e-01	1.99e-02	1.56	14	0.141	0.50	-0.12	1.23	-0.14	0.611
Recovery vs Vol 3%	4.25e-01	1.51e-02	3.77e-01	2.24e-02	7.71	14	p < 0.001	2.44	1.85	3.55	0.31	0.254
Recovery vs Burst-Supp	4.25e-01	1.51e-02	3.47e-01	1.81e-02	13.46	14	p < 0.001	4.51	3.58	6.66	-0.02	0.954

TABLE S5. Statistical results for cognitive matching from NeuroSynth in the sevoflurane dataset, using the Desikan-Killiany anatomical atlas.

Contrast	Baseline Mean	Baseline SD	Altered Mean	Null SD	tStat	df	pVal	Eff Size	95% CI Lower	95% CI Upper	Motion corr	Motion pVal
Awake vs Vol 2%	3.59e-01	8.34e-03	3.44e-01	9.36e-03	5.28	14	p < 0.001	1.63	1.02	2.60	0.14	0.611
Awake vs Vol 3%	3.59e-01	8.34e-03	3.26e-01	9.65e-03	11.44	14	p < 0.001	3.50	2.70	5.16	0.41	0.130
Awake vs Burst-Supp	3.59e-01	8.34e-03	3.20e-01	1.26e-02	8.90	14	p < 0.001	3.44	2.51	5.47	0.17	0.549
Recovery vs Vol 2%	3.47e-01	8.65e-03	3.44e-01	9.36e-03	1.00	14	0.336	0.32	-0.31	1.00	-0.19	0.507
Recovery vs Vol 3%	3.47e-01	8.65e-03	3.26e-01	9.65e-03	7.06	14	p < 0.001	2.19	1.69	3.05	0.23	0.411
Recovery vs Burst-Supp	3.47e-01	8.65e-03	3.20e-01	1.26e-02	6.27	14	p < 0.001	2.34	1.61	3.75	-0.09	0.763

TABLE S6. Statistical results for BrainMap decoding in the sevoflurane dataset

Contrast	Baseline Mean	Baseline SD	Altered Mean	Null SD	tStat	df	pVal	Eff Size	95% CI Lower	95% CI Upper	Motion corr	Motion pVal
Awake vs Vol 2%	3.48e-01	1.20e-02	3.23e-01	1.99e-02	5.73	14	p < 0.001	1.45	0.99	2.24	0.26	0.340
Awake vs Vol 3%	3.48e-01	1.20e-02	2.67e-01	2.49e-02	12.93	14	p < 0.001	3.98	3.22	5.69	0.25	0.375
Awake vs Burst-Supp	3.48e-01	1.20e-02	2.22e-01	1.76e-02	23.63	14	p < 0.001	8.07	6.44	11.93	0.36	0.192
Recovery vs Vol 2%	3.29e-01	1.55e-02	3.23e-01	1.99e-02	1.03	14	0.318	0.29	-0.29	0.85	-0.11	0.705
Recovery vs Vol 3%	3.29e-01	1.55e-02	2.67e-01	2.49e-02	8.75	14	p < 0.001	2.86	2.24	4.04	0.23	0.404
Recovery vs Burst-Supp	3.29e-01	1.55e-02	2.22e-01	1.76e-02	18.81	14	p < 0.001	6.20	4.69	10.51	0.10	0.714

TABLE S7. Statistical results for cognitive matching from NeuroSynth in the sevoflurane dataset, using 200 cortical regions from the Schaefer atlas, and 32 subcortical regions from the Tian atlas.